RSC Advances

PAPER

View Article Online
View Journal | View Issue

Cite this: *RSC Adv.*, 2022, **12**, 23017

Grafting of the gold surface by heterocyclic moieties derived through electrochemical oxidation of amino triazole – an experimental and "*ab initio*" study†

Nimet Orqusha *

Surface modification of gold is accomplished by using the aminyl radicals formed through the electrochemical oxidation of the amino-triazole molecule dissolved in organic media (acetonitrile). The electrochemistry of the grafting process and the redox behavior of the grafted heterocyclic layer are similar to those of aliphatic amines. The presence of AT groups on the electrode surface was studied by cyclic voltammetry (CV) and electrochemical impedance spectroscopy (EIS) before and after the functionalization process to confirm and prove the formation of a layer on the surface. The capability of the modified surfaces for blocking redox reaction was assessed using a ferrocyanide–ferricyanide redox couple and displayed important differences. The redox probes display a decrease in electron transfer rate. The increase of the charge transfer resistance of the grafted layer is suggestive of a compact layer formation. Furthermore, the Au13 cluster was used to compute BDEs (bond dissociation energies) and a number of other important parameters such as bond strength and length of the interface, *etc.* These parameters were computed using ONTEP software (Order-N Total Energy Package), intended specifically for calculations on large systems, and it employs density functional theory (DFT) in the density matrix formulation.

Received 17th May 2022
Accepted 9th August 2022

DOI: 10.1039/d2ra03125f

rsc.li/rsc-advances

1. Introduction

Surface modification of materials is realized using various organic compounds that possess a special affinity, which enables an easy way to adjust the properties of the materials and add some new attractive functionality that can be explored for: corrosion protection,[1] chemical-,[2,3] and bio-sensors,[4,5] molecular electronics[6,7] energy conservation and conversion.[1,8–10] The electrochemical derivation of conductive surfaces by the oxidation of amines to give attached thin organic layers was first reported in 1990 for carbon fiber[11] and GC electrodes.[3] This method was the first example of electrochemically-assisted

Department of Chemistry, University of Prishtina "Hasan Prishtina", FNMS, str. "Nëna Tereze" nr. 5, 10000 Prishtina, Republic of Kosovo. E-mail: nimet.orqusha@uni-pr.edu; Tel: +38343597556

† Electronic supplementary information (ESI) available. See https://doi.org/10.1039/d2ra03125f

Dr Sc. Nimet H. Orqusha was born on the 12.05.1984 in Prizren. She started her basic studies in the academic year 2002/2003 and graduated in 2006 from the University of Prishtina – Faculty of Mathematical and Natural Sciences (FMNS) in Engineering Chemistry where she received the title "Bachelor of Engineering Chemistry". In the academic year 2006/2007, she continued her studies in the Master program in – Organic Chemistry and Biochemistry, where in April 2010, she received the title "Master of Chemistry". The Doctoral Dissertation entitled: "Electrochemical modification of the surface of materials through 2D layers derived from triazoles: a joint experimental and theoretical study" was realized in collaboration between the University of Prishtina "Hasan Prishtina" and Umea University in Sweden, and as a result of this collaboration successfully defended her PhD thesis. On that occasion, she received the title "Doctor of Chemistry" in July 2021.

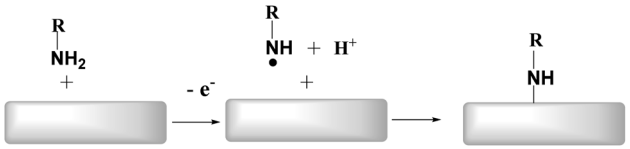

Scheme 1 General description of the modification of conductive surfaces by the oxidation of amines.

modification, which Pinson and co-workers established. The functionalization of surfaces was explored in detail with various organic compounds and electrode materials using this method. Aliphatic amines, which contain alkyl groups[2,4–6] and aromatic amines,[7] have been grafted at different carbon surfaces, including: GC,[5,7,11,12] PPF,[13] HOPG,[11] and carbon nanotubes (CNTs).[6]

In addition to carbon, the grafting method is also useful for modifying gold[14] and platinum substrates.[7] This technique's mechanism is based on the electrochemical formation of aminyl radicals[15] by the oxidation of the suitable amines that subsequently bind to the surface. Adenier and co-workers have explored the reaction and found that the surface grafting proceeds *via* a radical reaction.[7] The proposed and generally accepted reaction path is shown in Scheme 1.

The reaction proceeds *via* irreversible one-electron oxidation of the amine to form a radical cation. Finally, the radical cation deprotonates to give a carbon radical and an aminyl radical that subsequently binds to the surface.

Our study aim was to explore the grafting process and the stability of the layer through electrochemical and spectroscopic techniques. In this work, 3-amino-1,2,4-triazole (AT) is proposed for surface grafting of the gold electrode. The gold electrode was grafted with an AT layer *via* aminyl radical's formation under an electrochemical oxidation reaction.

The electrodes were characterized before and after the grafting by electrochemical impedance spectroscopy (EIS) cyclic voltammetry (CV) using ferro/ferricyanide as a redox probe to evaluate their barrier properties for electron transfer. X-ray photoelectron spectroscopy measurements (XPS) demonstrated immobilized AT at the electrode surface. In addition, atomic force microscopy (AFM) and ellipsometry were used to determine the grafted layer's thickness and morphology. The results indicate the AT groups' presence on the gold surface – confirming a successful grafting reaction. Through density functional theory (DFT) calculations, we understand that the bond between gold and the attached amino-triazole moiety is relatively stable.

2. Materials and methods

2.1 Reagents

All aqueous solutions used throughout this research were made with reagent-grade water (18 MΩ cm) using Milli-Q water (Q-POD's Millipore system, Darmstadt, Germany), and Q-POD's Millipore water system provided electrode cleaning. The solvents and reagents listed below were used as received without any further purification: ethanol (EtOH, 99.9%), acetonitrile (ACN, 99.9%), HPLC grade was obtained from Ficher Scientific (Bishop Meadow, Loughborough, UK), 3-amino-1,2,4 triazole were purchased from Sigma Aldrich (St. Louis, MO, USA), potassium ferrocyanide ($K_4[Fe(CN)_6]\cdot 3H_2O$) and potassium ferricyanide ($K_3[Fe(CN)_6]$), potassium chloride and tetrabutylammonium tetrafluoroborate (NBu_4BF_4).

Gold plate electrodes were purchased from Arrandee (Werther/Westfalen, Germany), specifically (2500 ± 500) Å thick gold film glazed with a 25 ± 15 Å chromium layer on borosilicate glass support (1.1 × 1.1 cm).

The gold electrode discs (Au, 0.2 cm diameter) were acquired from CH Instruments, Inc. Austin, TX. The USA.

2.2 Electrode preparation and modification

Au electrodes of two types were employed in this work, one was an Au rod electrode (d = 0.2 cm) for electrochemical analysis (CV, chronoamperometry, and EIS), and another was an Au plate for surface characterization (X-ray photoelectron spectra-XPS, ellipsometry, and atomic force microscopy).

Before the surface modification, the gold electrode surface was cleaned by polishing with a 1.0 micron alumina slurry (Buehler, Esslingen, Germany) and washed with water before the modification. After removal of trace alumina from the surface by rinsing with Milli-Q water and quick cleaning in an ultrasonic bath consisting of both ethanol and water (5 min each), electrochemical cleaning in 0.5 M H_2SO_4 by cycling between −0.3 and +1.5 V at 100 mV s^{-1} was carried out until a reproducible voltammogram was obtained. Before derivatization, the cleaned electrode was finally rinsed with Milli-Q water.

The electrochemical modification of the Au surface was carried out in an acetonitrile solution containing the AT and NBu_4BF_4, as described in Section 2.3. The electrochemical oxidation was operated with a cyclic scan at a potential range between +0.2 and +1.6 V *vs.* SCE under vigorous stirring, which was deaerated by bubbling with ultra-pure nitrogen gas for t = 5 min before each experiment. The stirring was turned off a few seconds before the electrochemical experiment.

The resulting Au/grafted electrode was abundantly rinsed with Milli-Q water sonicated in acetonitrile for 2.5 min. and rinsed again with Milli-Q water. The surface modification procedures of gold plates for the characterization studies were identical to those used for the electrochemistry measurements.

2.3 Preparation of 3-amino-1,2,4-triazole

Briefly, the surface modification of gold was carried out in 20 ml acetonitrile solution containing the AT (2 mM) and NBu_4BF_4 (50 mM) as the base electrolyte. The AT solution was generated at room temperature in the electrochemical cell under vigorous stirring (5 min).

2.4 Instrumentation and procedure

2.4.1 Electrochemical measurement. All electrochemical measurements were realized with a Modulab electrochemical system, ECS (Solartron Analytical, Farnborough, UK), and a conventional three-electrode system; respectively, bare and

modified Au electrodes were employed as a working electrodes, whereas Ag/AgCl (saturated KCl) as reference electrode and Pt wire were used as a counter electrode. All potentials were reported *versus* the Ag/AgCl reference electrode at room temperature. 5.0 mM $Fe(CN)_6^{3-/4-}$ in 100 mM KCl was used as a redox probe to investigate the Au-electrode, both before and after modification, using EIS and CV.

Electrochemical impedance spectroscopy (EIS). Electrochemical impedance spectroscopy characterized the electrode before and after the grafting process. An *ac* voltage of 10 mV in amplitude, using a frequency range from 65 kHz–0.5 Hz, was superimposed on the *dc* potential and applied to the studied electrode. The *direct* potential was always set up at the formal potential of $Fe(CN)_6^{3-/4-}$. Experimental data of electrochemical resistance plots were analyzed with Zview2 software. Zview2 software (version 3.4e) was used for equivalent circuit fitting and modeling.

Cyclic voltammetry (CV). CV was used both for electrochemical modification and for characterization of the modified electrode. Electrochemical oxidation of heterocyclic amine was characterized by cyclic voltammetry in ferricyanide/ferrocyanide (5.0 mM $Fe(CN)_6^{3-/4-}$ in 100 mM KCl) as a redox probe to evaluate their barrier properties for electron transfer. Cyclic Voltammetry was made in the range of +0.6 to −0.5 V at a scan rate of 100 mV s^{-1}.

2.4.2 Surface characterization of amino-triazole (AT) films on gold

Ellipsometry. Ellipsometry has also been used for determining the film thickness[12] and its refractive index. It has been proposed that ellipsometry can be applied to film thicknesses from monoatomic to a micrometer. The thicknesses of the AT film on the Au electrode (dried under N_2 flow after electrografting) were performed using a spectrometric ellipsometer (J. A. Woollam Co., Inc. (Lincoln, NE. USA)) alfa – SETM. The experiments were performed at an incident angle of 70°, spectral range 380 nm to 900 nm, and 180 wavelengths. Obtained spectra were analyzed using Complete Ease software.

Ellipsometric measurements were taken on the exact location of the sample plates before and after electrografting. The average and the standard deviation values reported agree with data points obtained from measuring five spots on each plate.

Atomic force microscopy. The surface morphology of the AT-modified Au electrode and the bare gold electrode were studied with AFM (Veeco, Plainview, NY, USA) NanoScope III fitted with a 125 m scanner (J-scanner) equipment. In addition, the NanoScope v720 software was employed for image processing and surface roughness calculations.

Each AFM image presented is representative of numerous images taken at different locations of the sample. The layer thickness was determined by comparing the profile heights between the modified and unmodified areas.

X-ray photoelectron spectroscopy (XPS). The XPS spectra were gathered using a Kratos Axis Ultra DLD electron spectrometer (Kratos Analytical Ltd, Manchester, UK) using a monochromated Al Kα source operated at 150 W.

Survey spectra were gathered at binding energies ranging from 1100 to 0 eV, at pass energy of 160 eV, and high-resolution spectra for photoelectron lines N 1s, C 1s, and Au 4f were gathered at pass energy of 20 eV. In addition, the binding energy (BE) scale was referenced to the Au 4f7/2 photoelectron line, set at 84.0 eV. The spectra were handled with the Kratos software (version 2.2.9).

Computational details. For density functional theory (DFT) calculations was used DMol3 (BIOVIA) software. DFT calculations were performed to shed light on the molecular level regarding the grafting reaction, geometry and the bond dissociation energy of the grafted moieties. The Au13 cluster was used to compute BDE (Bond dissociation energies) and several other important parameters such as bond strength and length of the interface. These parameters were computed using ONTEP[16] software [Order-N Total Energy Package – a software explicitly intended for calculations on large systems, it employs density functional theory (DFT) in the density matrix formulation]. GULP[17] software was also used to compute BDE of attached amino-triazole moiety on a range of increasing size gold clusters.

3. Results and discussion

3.1 Modification procedure and Au deposition

We employed CV to perform the grafting of AT on the Au electrode. The AT moiety attachment onto the Au electrode was carried out by the electrochemical oxidation of the corresponding 3-amino-1,2,4 triazole in ACN. The electrochemical oxidation was performed by cyclic voltammetry with a potential range between +0.2 and +1.6 V *vs.* SCE.

The CV scan obtained at Au (Fig. 1) shows a broad irreversible oxidation peak, approximately at 1.35 V on the first scan, which can be assigned to forming the aminyl radical that couples to the electrode surface. On the second scan, the wave shifted to more positive values, and the maximum current decreased gradually with the initial repeated scans because of the grafting of the AT moiety on the gold surface. However, on the fifth scan, this peak is absent, indicating the blocking of the

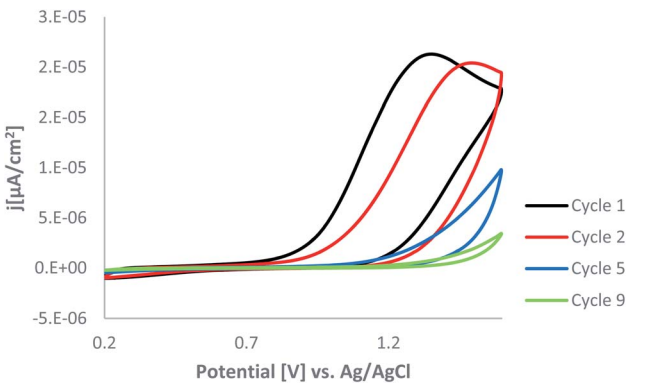

Fig. 1 Cyclic voltammograms recorded at the gold electrode with diameter d = 0.2 cm immersed in 3-amino-1,2,4-triazole (2 mM) solution after addition of (50 mM) NBu_4BF_4 to 20 ml acetonitrile. Scanning potential v = 100 mV s^{-1} and applied potential range from +0.2 to +1.6 V [black (first cycle), red (second cycle), blue (fifth cycle), green (ninth cycle)].

electrode surface. Finally, the CV current became nearly steady after five scans (it even disappeared), indicating the blocking of the Au surface with AT moieties. As this reaction proceeds, the surface becomes passivated. The binding of an AT layer to the surface of the electrode slows down the electron transfer and increases the difference of peak potentials (ΔE_p) of a reversible system in solution.

3.2 Characterization of the grafted layers by electrochemical measurements

3.2.1 Cyclic voltammetry using the redox probe, $Fe(CN)_6^{3-/4-}$. The surface modification has been accomplished by cyclic voltammetry through the electro-oxidation of amino-triazole using acetonitrile as a solvent. In addition, the presence of AT groups on the electrode surface was studied by cyclic voltammetry (CV) before and after the functionalization process to approve a layer's formation on the surface.

The capability of the modified surface for blocking redox reaction was assessed using the ferrocyanide–ferricyanide redox couple and displayed essential differences. First, the redox probes display a decreased electron transfer rate.

Fig. 2 shows that the bare Au electrode presents a quasi-reversible redox behavior attributed to the reduction and oxidation of the $Fe(CN)_6^{3-/4-}$ redox probes. On the other hand, the AT-modified electrode reveals a considerably blocking behavior for oxidation and reduction reactions of the $Fe(CN)_6^{3-/4-}$ redox system, and the electrochemical responses for the $Fe(CN)_6^{3-/4-}$ redox system is affected. Furthermore, it is apparent that after the modification of the gold electrode through the oxidation of AT, no peak was detected within the scanned potential window, which could be attributed to the blocking behavior of the modified surface.

The deposited layer affects the cyclic voltammogram, and the difference between the anodic and cathodic peak potentials (E_p) is increased, and Irel values are decreased. Fig. 2 shows that the blocking effect is significant, indicating that the grafting is quite efficient, and a layer of chemisorbed AT molecules almost entirely covers the Au surface. The electrochemistry of the grafting process and the redox behavior of the grafted amino-heterocyclic layer are similar to that of aliphatic amines.[2,7,18]

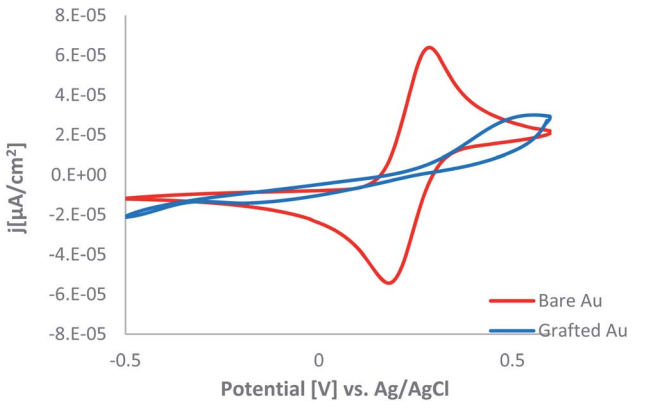

Fig. 2 Cyclic voltammograms recorded in aqueous solution of ferricyanide/ferrocyanide ions (5.0 mM $Fe(CN)_6^{3-/4-}$ in 100 mM KCl) on bare and modified gold electrode (modification by cyclic voltammetry, at potential range from +0.2 V to +1.6 V).

3.2.2 Electrochemical impedance spectroscopy of AT modified Au electrode using the redox probe, $Fe(CN)_6^{3-/4-}$. The electrochemical impedance spectroscopy measurements can evaluate the effect of 3-amino-1,2,4-triazole on the kinetics of a redox reaction at the gold electrode. The electrochemical behavior of the resulting AT modified electrode was investigated in the presence of an electroactive $Fe(CN)_6^{3-/4-}$ redox probe. In addition, this method has been used to confirm and determine the barrier properties of the deposited layer.

Superimposed Nyquist plots for the bare and modified gold electrodes; Equivalent circuits used to examine the impedance data for the bare (a) and modified (b) electrodes are presented in Fig. 3.

The Nyquist plot for the bare gold electrode shows the expected form of a faradaic impedance spectrum for conductive electrodes, at high frequencies (122.8 ohm domain) small semicircle characteristic of an interfacial charge-transfer mechanism, followed by a straight Warburg line 45° at low frequencies representing the diffusion-limited electron transfer process at the surface of the electrode. This response is typical of a simple redox $Fe(CN)_6^{3-/4-}$ reversible reaction.

The impedance plot for the gold electrode modified by electrochemical oxidation of AT differs considerably from that of the bare electrode.

The diameter of the semicircle raised significantly (R_{ct} = 1285 ohm), giving a surface coverage of 90.44% [eqn (1)]. This indicates that a compact blocking film slows down the probe's redox reaction, evidenced by CV (Fig. 2). The semicircle diameter determines the redox reaction's charge transfer resistance (R_{ct}) and the grafted layer's blocking properties. The increase of R_{ct} with electrolysis time demonstrates that the films become more compact. Qualitatively, the semicircle increase indicates that the electrode kinetics become slower as the gold electrode is modified with a substituted heterocyclic group. The Warburg line is observed for the modified electrodes in 65 kHz to 0.5 Hz.

The diffusional characteristics and the electron kinetics have been derived by modeling the EIS spectra with an equivalent electrical circuit (see inset in Fig. 3B) for both bare and modified electrodes, which comprises the solution resistance R_Ω, the charge-transfer resistance R_{ct}, the Warburg impedance W and the capacitance of the coated layer (Table 1).

Also, the increase in the charge-transfer resistance can be related to the electrode coverage and is given by the following equation:[19]

$$(1 - \theta) = R_{ct}^0/R_{ct} \quad (1)$$

The charge-transfer resistance calculated from the semicircle diameter increases dramatically following modification of the gold electrode surface from the value of 122.8 Ω for the bare electrode to 1285 Ω after electrochemical modification of gold by using the aminyl radicals formed through the electrochemical oxidation of the amino-triazole molecule dissolved in organic media. The raised charge transfer resistance of the

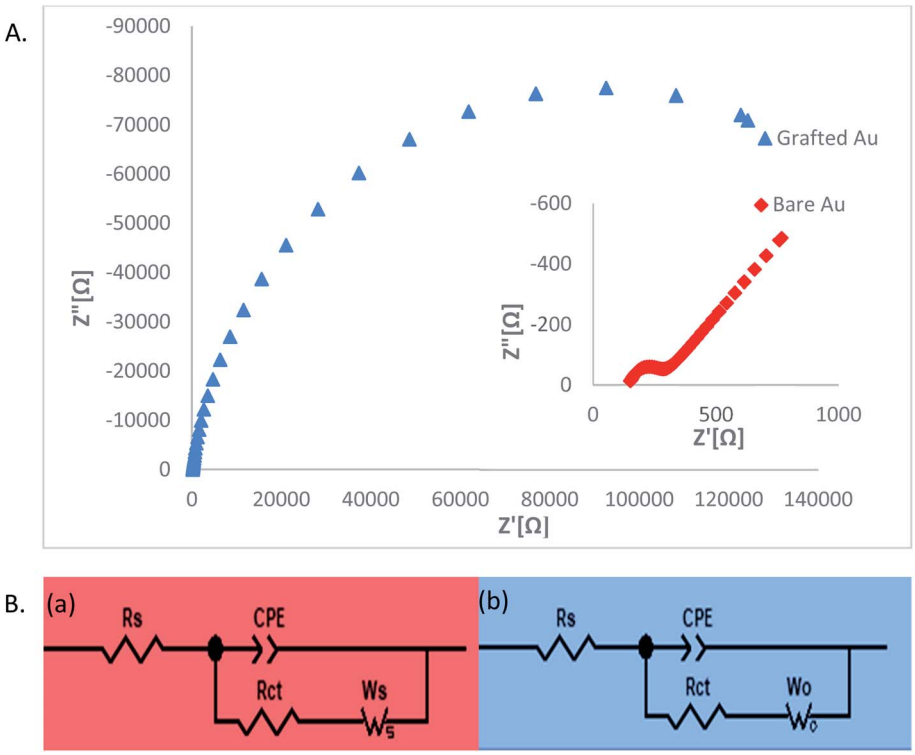

Fig. 3 (A) Electrochemical impedance spectroscopy (EIS) recorded in an aqueous solution of ferricyanide/ferrocyanide ions (5.0 mM $Fe(CN)_6^{3-/4-}$ in 100 mM KCl), 65 kHz–0.5 Hz frequency range, 10 mV ac-amplitude and 0.235 V dc potential on the bare and modified gold electrode with 3-amino-1,2,4-triazole (modification through cyclic voltammetry, applied potential range from +0.2 V to +1.6 V). (B) Equivalent circuits were used for electrochemical impedance data analysis for bare (a) and modified electrode (b).

grafted layer is suggestive of a compact layer formation. As can be observed, surface coverage close to 91% was obtained, indicating that the AT film covers almost the entire surface.

3.3 Ellipsometry

Spectroscopic ellipsometry was used for characterizing film thickness and refractive index. The optical thickness was dictated using a built-in model available in the Complete Ease software, *i.e.*, for bare Au electrode was used model B-Spline with starting material Au, while for the grafted layer was used the model WvlByWvl. Ellipsometric measurements were carried out on the same area of the plates before and after electrografting.

Because the measurements were carried out on dried and therefore collapsed films, the layer's refractive index was set at a constant value (real = 1.50; imaginary = 0), independent of its thickness.

Table 2 The thickness of the grafted layer on the gold electrode surface was obtained from the average measurements done on five different spots on each plate.[20]

Measurements	1-st	2-nd	3-rd	4-th	5-th
Thickness (nm)	4.0	4.2	3.2	3.5	3.5
Average	3.7 nm				

The thickness of the grafted layer on the surface of the gold electrode accounted for the average value of the five measurements was ~(3.7 ± 0.4 nm). Therefore, the layer thickness data obtained from ellipsometry and AFM measurements correlate well (Table 2).

Table 1 The EIS fitting parameters obtained using the equivalent circuits presented in Fig. 3B and the corresponding apparent fractional coverage (θ) calculated by eqn (1) in the solution (2 mM) of 3-amino-1,2,4-triazole after addition of (50 mM) NBu_4BF_4 to 20 ml acetonitrile[a]

Bare Au	Chi-Sqr	Sum-Sqr	R_s	CPE-T	CPE-P	R_{ct}	Ws-R	Ws-T	Ws-P	θ %
	2.39×10^{-5}	0.00194	159.9	3.39×10^{-6}	0.85884	122.8	3580	8.453	0.49721	—
Grafted Au	Chi-Sqr	Sum-Sqr	R_s	CPE-T	CPE-P	R_{ct}	Wo-R	Wo-T	Wo-P	θ %
	0.000113	0.009175	167.2	1.32×10^{-6}	0.91148	1285	2188	3.00×10^{0}	0.51727	90.44

[a] R_s – solution resistance; R_{ct} charge-transfer resistance; CPE-T – is a pseudocapacitance which is called Q, CPE-P – is related to the semicircle in nyquist plot (depressed semicircle), normally used the notation 'n' by using CPE-P and CPE-T and resistance one can calculate the true capacitance for the electrodes; (WO-R, WO-T, and WO-P) are three parameters of the Warburg resistance and θ – electrode coverage.

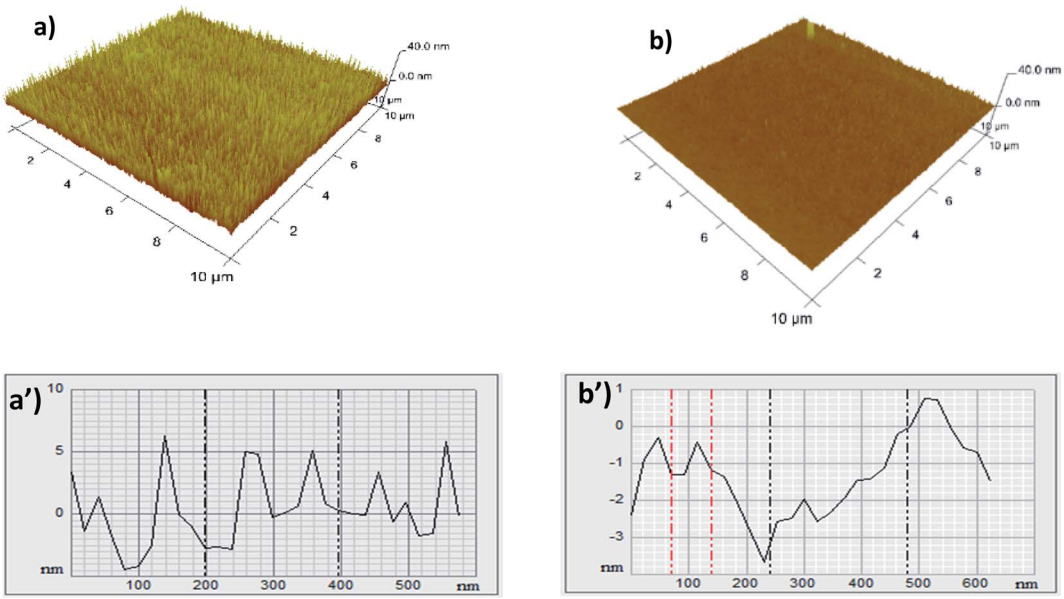

Fig. 4 Atomic force microscopy images (AFM) of the 3D surface and the roughness profile (a and a′ – modified gold electrode); and (b and b′ – bare gold electrode).

3.4 Surface characterization of AT-modified Au electrodes by AFM

AFM is a model of scanning probe microscopy with exhibited resolution on the order of fractions of a nanometer, more than 1000 times superior to the optical diffraction limit. A mechanical probe gathers the information by "touching" the surface. Height images were collected in the tapping mode. The thickness of the layer was found by comparing the profile heights between modified and unmodified areas. Nanoscope v720 software was used for the analysis of images (Fig. 4).

Surface modification of gold using the aminyl radicals formed through the electrochemical oxidation of the amino-triazole molecule is evidenced.

The AFM images of amino-heterocyclic modified electrodes clearly show that the electrodes' surfaces are covered with a granular AT layer. Furthermore, the granular features of the electrode modified by using cyclic voltammetry (several scan cycles in the potential range +0.2 and +1.6 V) through the electro-oxidation of AT dissolved in organic media were uniform with a (3.8 ± 0.2 nm) average diameter, which is in good agreement with the ellipsometric measurements (~3.7 ± 0.4 nm).

These results indicated that the electrochemical process yields films much thicker than one monolayer (considering that the thickness of the single amino-triazole molecule is ~0.35 nm). This shows a multilayer film composed of at least 11 amino-triazole moieties.

3.5 XPS characterization of modified Au electrodes

The surface analysis by X-ray photoelectron spectroscopy (XPS) is given and discussed below to determine the electronic properties and estimate the surface concentration of AT moieties formed on the gold surface. In addition, XPS analysis was used to investigate the composition of the organic adsorbed layer on the gold surface. As a result, the bare gold surface spectrum presents only the expected peaks, including binding energy of 84.0 eV attributed to Au 4f7/2.

Traces of carbon at 284.2 eV; 285.8 eV; 288.5 eV (C 1s) and oxygen at 530.8 eV; 532.4 eV (O 1s) are detected, which is probably due to the adsorption of organic contaminants during the cleaning process in a basic Piranha solution.

After grafting the AT on the gold surface, the Au and oxygen peak intensities decreased significantly, whereas carbon and nitrogen increased. A notable decrease of the Au 4f peak from (54.79 at%) in the bare gold surface down to (22.41 at%) in the grafted electrode upon surface modification with AT groups can be due to film formation, which masks the signal of Au 4f7/2.[18] This agrees with the electrochemical data and suggests that a layer was deposited.

Table 3 Atomic concentrations (at%) of distinct elements at the Au electrode surface after modification with AT layer

	BE, eV	AC, at%	at% per Au	BE, eV	AC, at%	at% per Au
Line	Unmodified Au			Modified AT/Au		
C 1s	284.2	29	52.92	284.6	9.5	42.39
	285.8	4.94	9.01	286.3	11.03	49.21
	287.1	2.9	5.29	287.8	16.86	75.23
	288.5	1.4	2.55			
O 1s	530.8	4.26	7.77	531.3	3.24	14.45
	532.4	2.73	4.98	532.6	7.27	32.44
N 1s	—	—	—	399.3	22.52	100.49
	—	—	—	401.1	7.18	32.03
Au 4f7/2	84	54.79	100	84	22.41	100

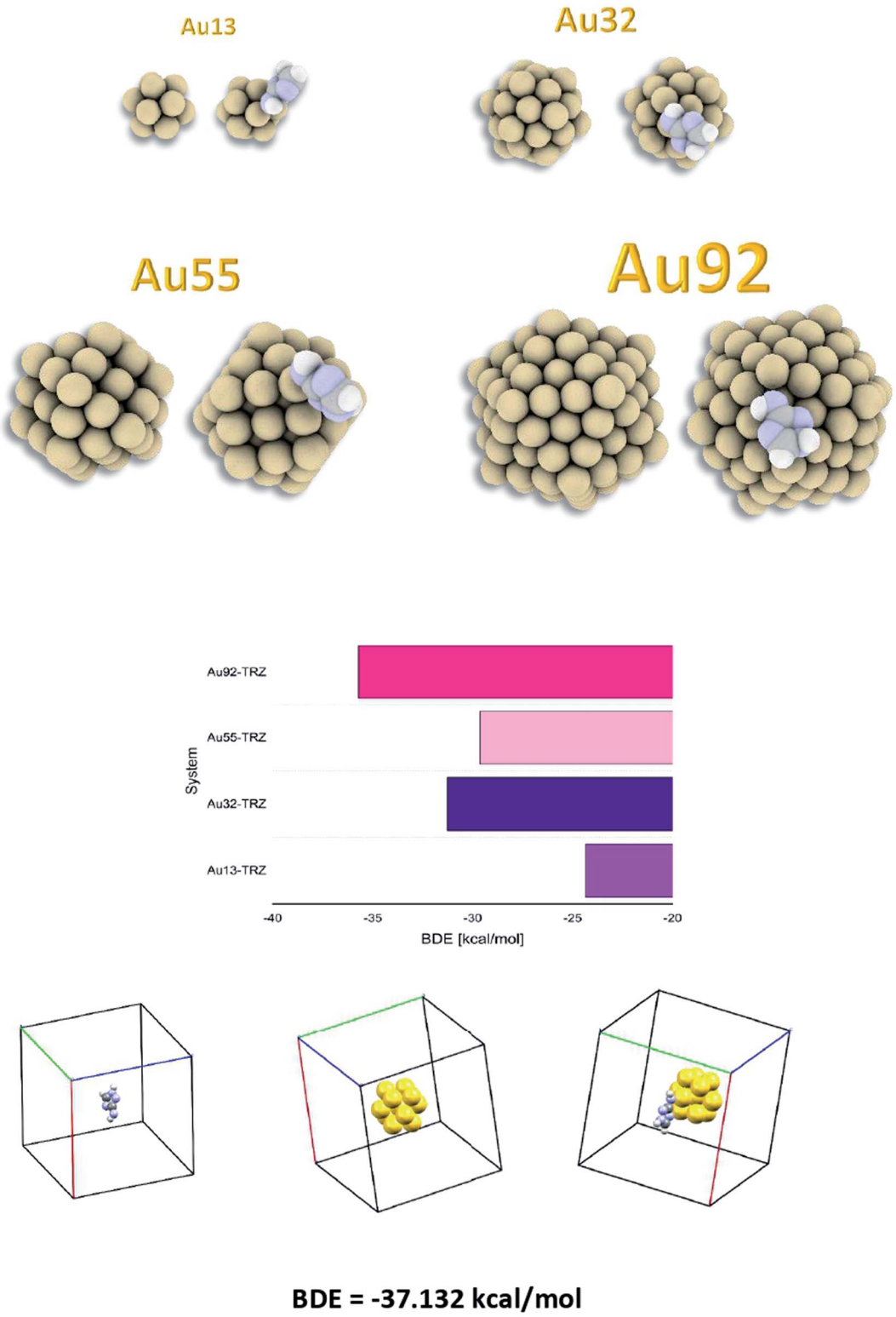

Fig. 5 Grafted gold clusters (Au13, Au32, Au55 and Au92); corresponding dissociation energies (BDE) Au-TZ and the BDE calculations scheme (optimized structures).

Following ultrasonic treatment, the N 1s core level spectra were measured for gold electrodes modified with AT. The N 1s spectrum of the AT modified electrode can be fitted with two peaks at 399.3 eV and 401.1 eV. The peaks at 399.3 (22.52 at%)[21–23] and 401.1 eV (≈7.18 at%) are ascribed to the aromatic nitrogen of the ring (=N–)[21–24] and protonated or hydrogen-bonded nitrogen (are ascribed to the –NH bond).[25]

The total atomic percentage of nitrogens on the ring is (≈29 at%).

The C 1s component at 287.8 eV is ascribed to carbon attached to the nitrogen group (N=C–N) in the triazole ring (13.96 ≈ 14 at%)[26] (after deducting the percentage of impurity). In conclusion, the ratio of nitrogen/carbon in the ring is approximately 4 to 2, following the atomic percentage of (≈29 at%) N with (≈14 at%) C.

These peaks confirm the presence, at the surface of the electrode, of the functional groups associated with the corresponding AT species. The obtained results suggest that the gold electrode was grafted with an AT layer *via* aminyl radicals' formation under an electrochemical oxidation reaction.

A more detailed analysis of the modified Au electrode's surface composition can be obtained from the core level spectra, and the atomic surface concentrations (at%) obtained by the integration of the core level peaks are summarized in Table 3.

After modifying the gold surface with AT molecules, the Au and oxygen peak intensities decreased obviously.

For the modified layer, compared to the bare, an increase in the content of carbon and nitrogen (per Au) was observed throughout the C 1s and the N 1s regions: *e.g.*, peak intensities for carbon at 287.1 eV attached to the nitrogen group (N–C–N) in the triazole ring increased from (5.29) up to (75.23).

Also, new peaks have appeared at 399.3 eV and 401.1 eV for protonated or hydrogen-bonded nitrogen (–NH). The grafted electrode, has greater loadings of nitrogen and carbon species resulting from the aminotriazole overlay.

3.6 DFT

The bond dissociation energy (BDE) between the Au13, Au32, Au92, and Au55 gold cluster and the grafted amino triazole moiety in a vacuum, together with the BDE scheme (optimized geometry in the vacuum), is presented in Fig. 5.

Theoretical calculations (performed using GULP) on different sized Au clusters (Au13 − Au92) show that the formed interface between gold and the attached triazole moiety is quite stable (BDE for Au92-TRZ is −37.5 kcal mol^{-1}). The same range of BDE is found also using a more precise calculations using ONTEP (BDE = −37.13 kcal mol^{-1}).

4. Conclusions

The results presented in this work support that the amine-triazole (AT) groups have been successfully deposited on a gold electrode. The modification involves a one-electron oxidation reaction in which the amino group of AT is converted to a reactive aminyl radical that binds to the Au surface through a carbon–nitrogen bond.

The electrochemical grafting of AT groups on a gold surface was further investigated and characterized by several techniques such as cyclic voltammetry (CV), impedance spectroscopy (EIS), ellipsometry, and atomic force microscopy (AFM), and X-ray photoelectron spectroscopy (XPS). The modified surface's ability to block redox reaction was evaluated using $Fe(CN)_6^{3-/4-}$ reversible redox probe and revealed essential differences. The redox probes show a decreased electron transfer rate (current decrease and enlargement of peak splitting of I_c and I_a) compared with the bare electrode signal. Charge transfer resistance increases dramatically following the gold electrode surface modification from a value of 122.8 Ω for the bare electrode to 1285 Ω after electrochemical modification by cyclic voltammetry in the potential range +0.2 and +1.6 V through the electro-oxidation of AT. An increase in RCT indicates that the permeability of the films to the redox probe becomes low. This also verifies that the film structures are more compact, which will prevent an easy exchange of the probe between the interior of the film and the solution.

AFM and ellipsometry measurements confirmed the formation of multilayer films. In addition, the AFM images of amino heterocyclic-modified electrodes clearly show that the electrodes' surfaces are covered with a granular ∼3.8 average diameter, which is in good accordance with the ellipsometric measurements ∼3.7. These results suggest that the electrochemical process yields thicker films than one monolayer.

XPS studies confirmed the electrochemistry results. After electrochemical derivatization, the intensities of the Au peaks decreased remarkably. A remarkable decrease of the Au4f peak upon surface modification with AT groups can be explained due to uniform film formation. Theoretical calculations (performed using GULP) on different sized Au clusters (Au13 − Au92) show that the formed interface between gold and the attached amino-triazole moiety is relatively stable (BDE from Au92-TRZ is −37.5 kcal mol^{-1}). The same BDE range is also found using more precise calculations using ONTEP (BDE = −37.13 kcal mol^{-1}).

Author contributions

Conceptualization, N. O.; investigation, experiments, N. O.; writing—original draft preparation, N. O.; writing—review and editing, N. O.

Conflicts of interest

The author declares no conflict of interest.

Acknowledgements

N. O. acknowledges the support from Erasmus plus (Project: Development of an advanced and applied course in electrochemistry with flexible and creative learning), and I am also grateful to the University of Umea for helping me accomplish the experimental part of this work.

References

1 S. Rengaraj, P. Kavanagh and D. Leech, *Biosens. Bioelectron.*, 2011, **30**, 294–299.
2 J. Pinson, G. Desarmot and M. Sanchez, *J. Electrochem. Soc.*, 1990, **137**(6), 1757–1764.

3 A. Hjarbæk, K. Højrup, B. Winther-jensen, S. Uttrup and K. Daasbjerg, *Electrochim. Acta*, 2007, **53**, 1680–1688.
4 R. S. Deinhammer, M. Ho, J. W. Anderegg and M. D. Porter, *Langmuir*, 1994, **10**, 1306–1313.
5 A. C. Cruickshank and A. J. Downard, *Electrochim. Acta*, 2009, **54**, 5566–5570.
6 L. Yang, J. Chen, X. Wei, B. Liu and Y. Kuang, *Electrochim. Acta*, 2007, **53**, 777–784.
7 A. Adenier, M. M. Chehimi, I. Gallardo, J. Pinson and N. Vila, *Langmuir*, 2004, **20**(19), 8243–8253.
8 X. Wang, A. Dong, Y. Hu, J. Qian and S. Huang, *RSC Adv.*, 2020, **56**, 10809–10823.
9 F. Ran, X. Xu, D. Pan, Y. Liu, Y. Bai and L. Shao, *Nano-Micro Lett.*, 2020, **12**, 46.
10 X. Li, C. Hao, B. Tang, Y. Wang, M. Liu, Y. Wang, Y. Zhu, C. Lu and Z. Tang, *Nanoscale*, 2017, **9**, 2178–2187.
11 M. Tanaka, T. Sawaguchi, Y. Sato, K. Yoshioka and O. Niwa, *Langmuir*, 2011, **27**, 170–178.
12 Y. S. Sun, *Instrum. Sci. Technol.*, 2014, **42**, 109–127.
13 R. Nasraoui, J. Bergamini, S. Ababou-Girard and F. Geneste, *J. Solid State Electrochem.*, 2011, **15**, 139–146.
14 J. Zhang, L. Mou and X. Jiang, *Chem. Sci.*, 2020, **11**, 923–936.
15 I. Gallardo, J. Pinson and N. Vila, *J. Phys. Chem. B*, 2006, **110**, 19521–19529.
16 C. Skylaris, P. D. Haynes, A. A. Mostofi and M. C. Payne, *J. Chem. Phys.*, 2005, **122**(8), 1–10.
17 P. Taylor, J. D. Gale and A. L. Rohl, *Mol. Simul.*, 2003, **29**, 291–341.
18 D. Bélanger and J. Pinson, *Chem. Soc. Rev.*, 2011, **40**, 3995–4048.
19 E. Sabatani and I. Rubinstein, *J. Electroanal. Chem.*, 1987, **91**, 6663–6669.
20 M. Lillethorup, M. Kongsfelt, M. Ceccato, B. B. E. Jensen, B. Jørgensen, S. U. Pedersen and K. Daasbjerg, *High- versus Low-Quality Graphene: A Mechanistic Investigation of Electrografted Diazonium-Based Films for Growth of Polymer Brushes*, Wiley-VCH Verlag GmbH Co. KGaA, Weinheim, 2014, vol. 10, pp. 922–934.
21 M. Tourabi, K. Nohair, M. Traisnel, C. Jama and F. Bentiss, *Corros. Sci.*, 2013, **75**, 123–133.
22 F. Bentiss, C. Jama, B. Mernari, H. El Attari, L. El Kadi, M. Lebrini, M. Traisnel, M. Traisnel, M. Lagrenée and M. Lagrenée, *Corros. Sci.*, 2009, **51**, 1628–1635.
23 M. Traisnel, L. Gengembre, H. Vezin, F. Bentiss, M. Lagrené and M. Lebrini, *Appl. Surf. Sci.*, 2007, **253**, 9267–9276.
24 K. Akaike, K. Aoyama, S. Dekubo, A. Onishi, K. Kanai, K. Akaike, K. Aoyama, S. Dekubo, A. Onishi and K. Kanai, *Chem. Mater.*, 2018, **30**(7), 2341–2352.
25 S. A. John, S. Kesavan and P. Arunachalam, *RSC Adv.*, 2014, **4**, 30896–30905.
26 C. I. Sathish, S. Premkumar, X. Chu, X. Yu, M. B. H. Breese, M. Al-abri, A. H. Al-muhtaseb, A. Karakoti, J. Yi and A. Vinu, *Angew. Chem.*, 2021, **60**, 21242–21249.